

1
2
3
4 MC3T3-E1 and RAW264.7 cell response to hydroxyapatite and alpha-type alumina adsorbed
5
6
7 with bovine serum albumin
8
9

10
11
12 Masakazu Kawashita¹, Jumpei Hayashi¹, Tada-aki Kudo², Hiroyasu Kanetaka³, Zhixia Li⁴,
13
14
15 Toshiki Miyazaki⁵ and Masami Hashimoto⁶
16
17

18
19
20
21 ¹ Graduate School of Biomedical Engineering, Tohoku University, Sendai 980-8579 Japan
22

23
24 ² Graduate School of Dentistry, Tohoku University, Sendai 980-8575 Japan
25

26
27 ³ Liaison Center for Innovative Dentistry, Graduate School of Dentistry, Tohoku University,
28
29
30 Sendai 980-8575 Japan
31

32 ⁴ College of Chemistry and Chemical Engineering, Guangxi University, Nanning 530004,
33
34 China
35

36
37 ⁵ Graduate School of Life Science and Systems Engineering, Kyushu Institute of Technology,
38
39
40 Kitakyushu 808-0196 Japan
41

42
43 ⁶ Japan Fine Ceramics Center, Nagoya 456-8587, Japan
44
45

46
47
48
49 *Corresponding author:

50
51
52 Masakazu Kawashita

53
54
55 Graduate School of Biomedical Engineering, Tohoku University

56
57
58 6-6-11-901-4 Aramaki-Aoba, Aoba-ku, Sendai 980-8579, Japan
59

1
2
3
4 TEL: +81-22-795-3937, FAX: +81-22-795-4735
5
6

7 E-mail: m-kawa@ecei.tohoku.ac.jp
8
9
10
11
12
13
14
15
16
17
18
19
20
21
22
23
24
25
26
27
28
29
30
31
32
33
34
35
36
37
38
39
40
41
42
43
44
45
46
47
48
49
50
51
52
53
54
55
56
57
58
59
60

Abstract

Initial cell responses following implantation are important for inducing osteoconductivity. We investigated cell adhesion, spreading, and proliferation in response to native and bovine serum albumin (BSA)-adsorbed disc of hydroxyapatite (HA) or alpha-type alumina (α -Al₂O₃) using mouse MC3T3-E1 osteoblastic cells and mouse RAW264.7 macrophages. The adsorbed BSA inhibited adhesion and spreading of MC3T3-E1 cells, but did not affect MC3T3-E1 cell proliferation on HA and α -Al₂O₃ substrates. Thus, MC3T3-E1 cells quickly adhere to original HA before cell binding is impeded by adsorption of BSA in quantities sufficient to inhibit the adhesion of MC3T3-E1 cells. The adsorbed BSA inhibits adhesion of RAW264.7 cells to α -Al₂O₃, but not to HA. BSA adsorption does not affect RAW264.7 cell spreading and proliferation on both HA and α -Al₂O₃ substrates. Thus, BSA adsorbed on HA stimulates a different cell response than α -Al₂O₃. Moreover, quick adherence of osteoblast cells and monocyte-macrophage lineage cells plays a role in HA osteoconductivity.

Keywords: MC3T3-E1, RAW264.7, hydroxyapatite, alumina, bovine serum albumin

1. Introduction

Osteoconductivity is the ability of biomaterials to support bone formation and chemically bond to bone. Hydroxyapatite (HA) [1,2] and alpha-type alumina (α -Al₂O₃) [3] are typical

1
2
3
4 osteoconductive and non-osteoconductive biomaterials, respectively. The process of
5
6
7 osteoconductivity occurs in six stages: (1) serum protein adsorption, (2) cell recruitment, (3)
8
9
10 cell attachment and proliferation, (4) cell differentiation and activation, (5) matrix
11
12
13 calcification, and (6) bone remodeling [4,5]. Post implantation, the biomaterials are
14
15
16 immediately coated with, and subsequently adsorb, layers of proteins from blood and tissue
17
18
19 fluids. Importantly, all subsequent cellular responses are dependent on the implants' ability to
20
21
22 adsorb protein at early time points [6,7]. However, a detailed mechanism of the
23
24
25 osteoconductive process is not yet clear.

26
27 To fully understand the osteoconductive mechanism, we have focused our attention on the
28
29
30 adsorption of albumin and osteopontin (OPN) on implanted materials. This is because they
31
32
33 are present at implant site and bind HA, which might affect the initial osteoblasts and
34
35
36 osteoclasts response. Recently, work from our lab has shown that the non-osteoconductive
37
38
39 alpha-type alumina ($\alpha\text{-Al}_2\text{O}_3$) exhibited a greater adsorption capacity for bovine serum
40
41
42 albumin (BSA) and OPN than osteoconductive HA [8]. No definitive correlation was
43
44
45 observed between albumin or OPN adsorption capacity and the osteoconductivity of materials,
46
47
48 suggesting that other factors (e.g., albumin and/or OPN orientation, and arrangement) likely
49
50
51 dictate the osteoconductive nature of implanted materials.

52
53 It is known that BSA is adsorbed on HA through ionic interactions between amino acids
54
55
56 residues containing COO^- groups and the Ca^{2+} sites on the HA surface [9]. Therefore, the
57
58
59

1
2
3
4 specific adsorption of BSA on HA could effectively mediate osteoblast cell adhesion. In fact,
5
6
7 heat-denatured BSA is effective at blocking MC3T3-E1 osteoblast-like cell adhesion of some
8
9
10 substrates [10], whereas it hardly influences the adhesion or proliferation of MC3T3-E1 cells
11
12
13 to HA [11].

14
15 Osteoclasts and osteoblasts play an important role in bone remodeling [12]. Osteoclast
16
17
18 formation occurs through the following mechanism: 1) osteoblasts produce macrophage
19
20
21 colony-stimulating factor (M-CSF) that induces the expression of receptor activator of the
22
23
24 nuclear factor- κ B (RANK) localized on the surface of monocyte-macrophage lineage cells
25
26
27 (precursor of osteoclasts); 2) RANK ligand (RANKL), which is present on cell surface of
28
29
30 osteoblasts, binds to RANK; and 3) RANKL interaction with RANK stimulates the
31
32
33 differentiation of precursors into multinucleated osteoclasts and activates osteoclasts [13,14].
34
35
36 Therefore, the initial adhesion of not only osteoblasts, but also monocyte-macrophage lineage
37
38
39 cells, might be important for osteoconductivity.

40
41 To date, no comparative studies have investigated the effect of BSA adsorption on the
42
43
44 osteoblasts response and production of monocyte-macrophage lineage cells in the presence of
45
46
47 osteoconductive HA and non-osteoconductive α -Al₂O₃. In this study, we examined the effect
48
49
50 of adsorbed BSA on the responses of osteoblast-like MC3T3-E1 cells and RAW264.7
51
52
53 macrophages. These findings will enhance our understanding of the osteoconductive
54
55
56 mechanisms of biomaterials with the goal of using this information to develop highly
57
58
59
60

1
2
3
4 osteoconductive biomaterials for medical implantation.
5
6
7

8 9 10 **2. Materials and Methods**

11 12 **2.1 Sample Preparation.**

13
14
15 Commercially available HA powder (HAP-200; Taihei Chemical Industrial Co. Ltd., Osaka,
16
17
18 Japan) was molded in a metal die and then cold isostatically pressed (CIP; MODEL 30X;
19
20
21 Kobe Steel, Ltd., Hyogo, Japan) at 245 MPa to form 14-mm diameter discs. To generate the
22
23
24 discs, they were sintered at 1300 °C for 1 h in air. For heating and cooling rates, 30 °C/min
25
26
27 was used for heat and furnace cooling was used to cool. For this study, 14-mm diameter
28
29
30 α -Al₂O₃ discs were purchased from a commercial supplier (SSA-S; Heat System Co. Ltd.,
31
32
33 Fukuoka, Japan). The discs were then polished with sandpaper (400 grit) to produce a uniform
34
35
36 surface roughness. Prior to experimentation, discs were washed with acetone, ethanol, and
37
38
39 distilled water. These discs are called “original discs” throughout the study.
40
41
42
43
44

45 **2.2 Sample Characterization.**

46
47 The crystalline phase of the original disc was examined with a thin film X-ray
48
49
50 diffractometer (XRD; RINT-2200VL; Rigaku Co. Ltd., Tokyo, Japan) under the following
51
52
53 settings: X-ray source, Ni-filtered CuK α radiation; X-ray power, 40 kV, 40 mA; scanning rate,
54
55
56 $2\theta = 2^\circ/\text{min}$; and sampling angle, 0.02° . Surface morphology and roughness measurements of
57
58
59
60

1
2
3
4 the original disc obtained using a scanning electron microscope (SEM; VE-8800; Keyence,
5
6
7 Tokyo, Japan). Statistical analysis was performed using the Student's *t*-test and *P*-values <
8
9
10 0.05 were considered significant.

11 12 13 14 15 **2.3 Measurement of Protein Adsorption.** 16

17
18 BSA (8 mg/ml) (Jackson Immuno Research Laboratories, INC., Pennsylvania, US) in 2 ml
19
20 of saline was adsorbed on original discs at 4 °C for 24 h. These discs are termed
21
22 BSA-adsorbed discs in this manuscript. The original and BSA-adsorbed discs were exposed to
23
24 1 ml of Dulbecco's Modified Eagle Medium (DMEM; Wako Pure Chemical Industries, Ltd.,
25
26 Osaka, Japan) supplemented with 20% fetal bovine serum (FBS; Life Technologies
27
28 Corporation, CA, US) for 1, 3 and 6 h at 37 °C. Notably, both original and BSA-adsorbed
29
30 discs were incubated in DMEM supplemented with FBS. The aim of this study is to
31
32 investigate the effect of BSA on cell responses. However, in the cell culture assay, we have
33
34 used DMEM supplemented with FBS, and this contains various kinds of proteins (mainly
35
36 BSA). Therefore, we must carefully consider the effects of proteins derived from the culture
37
38 medium in our cell culture assay. That is, if a large amount of protein in the culture medium is
39
40 quickly adsorbed on the discs and there is no difference in the amounts of adsorbed protein
41
42 between the original and BSA-adsorbed discs, it is difficult to determine any cell response
43
44 effects due to preliminarily adsorbed BSA. Therefore, both original and BSA-adsorbed discs
45
46
47
48
49
50
51
52
53
54
55
56
57
58
59
60

1
2
3
4 were incubated in DMEM supplemented with FBS for this study. After rinsing the unadsorbed
5
6 protein, adsorbed protein were homogenized in a RIPA lysis buffer comprised of 50 mM
7
8 Tris-HCl (pH8.0), 150 mM NaCl, 1% (v/v) Nonident P-40, 0.5% (w/v) sodium deoxycholate,
9
10 0.1% (w/v) sodium dodecyl sulfate (SDS), 0.2 mM dithiothreitol, 1 mM phenylmethylsulfonyl
11
12 fluoride, and a protease inhibitor cocktail (Roche Diagnostics, Indianapolis, IN, US). The
13
14 amounts of adsorbed protein were determined using the Bradford dye binding assay [15].
15
16
17
18
19
20
21
22 Statistical analysis was performed using the Student's *t*-test and *P*-value < 0.05 was
23
24 considered significant.
25
26
27
28
29

30 **2.4 MC3T3-E1 and RAW264.7 Cell Adhesion, Spreading, and Proliferation Assay.**

31
32
33 Original discs were autoclaved at 121 °C for 20 min and adsorbed with BSA at 8.0 mg/ml in
34
35 2 ml of saline at 4 °C for 24 h. Following BSA adsorption, the samples were transferred to a
36
37 24-well culture plate (Techno Plastic Product AG; Trasadingen, CH). Each disc was seeded
38
39 with 1×10^4 MC3T3-E1 osteoblast-like cells or RAW264.7 monocytic cells in 1 ml of
40
41 DMEM supplemented with 20% FBS and penicillin/streptomycin. For experiments, the cells
42
43
44
45
46
47 were cultured for various periods of time ranging from 1 h to 14 d at 37 °C and 5% CO₂.
48
49

50
51 For cell adhesion and spreading assays, cells adhered to discs were stained with fluorescein
52
53 diacetate (FDA; Dojindo Laboratories, Kumamoto, Japan), and the number of adhered cells
54
55
56
57 were counted and the maximum cell length was determined using an inverted fluorescent
58
59
60

1
2
3
4 microscope (CKX41, Olympus, Tokyo, Japan). To determine cell proliferation, we isolated
5
6
7 DNA from viable cells adhered to discs at 2, 7, and 14 d after incubation by using the AllPrep
8
9
10 DNA/RNA/Protein Mini Kit and QIA Shredder columns (Qiagen Inc., CA, USA), according
11
12
13 to the manufacturer's protocol. Cell extraction was performed using cell scrapers (Sumitomo
14
15 Bakelite Co. Ltd., Tokyo, Japan) and DNA was quantified by measuring absorbance at 260
16
17
18 nm by using a spectrophotometer (GeneQuant Pro; GE Healthcare, Buckinghamshire, UK).
19
20
21 Statistical analysis was performed using the Holm's test and P -values < 0.05 were considered
22
23
24 significant.
25
26
27
28
29

30 **3 Results and Discussion**

31 **3.1 Sample Structure**

32
33
34
35
36 Figure 1 shows the XRD patterns for (a) HA discs and (b) α -Al₂O₃ discs and the resulting
37
38
39 diffraction patterns were unique to HA and α -Al₂O₃. We also confirmed that no other
40
41
42 unexpected crystalline phase was contained in these samples, by examining the XRD patterns
43
44
45 for peaks other than that of HA and α -Al₂O₃. SEM images of (a) HA disc and (b) α -Al₂O₃
46
47
48 discs are shown in Figure 2. These images indicate that each disc exhibited a similar surface
49
50
51 morphology. The arithmetic mean of the height variation on the roughness profiles (Ra), the
52
53
54 distance between the highest and the lowest on the roughness profiles (Ry), and the ten-point
55
56
57 height of irregularities (Rz) are listed in Table 1. There was no statistically significant
58
59
60

1
2
3
4 difference in these parameters between HA and α -Al₂O₃ discs. These results suggest that any
5
6
7 difference in surface morphology and roughness between HA and α -Al₂O₃ discs that might
8
9
10 affect protein adsorption and the cell response can be considerable reduced.

11 12 13 14 15 **3.2 Effect of BSA Adsorption on Sample Behavior**

16
17
18 Figure 3 represents amount of adsorbed protein on (a) HA disc and (b) α -Al₂O₃ discs over
19
20
21 time. Protein was hardly detected on HA and α -Al₂O₃ discs before incubation (0 h), whereas
22
23
24 ~ 0.2 mg of protein was detected on BSA-adsorbed discs. In addition, the adsorbed amount of
25
26
27 protein hardly increased with longer incubation periods. This suggests that the surface of the
28
29
30 disc was almost saturated with BSA over an extremely short incubation period and that a
31
32
33 small amount of protein in the culture media was further adsorbed on the discs with increased
34
35
36 incubation time. We found that HA and α -Al₂O₃ discs were saturated with BSA at a
37
38
39 concentration of 1.0 mg/ml [8]. The concentration of BSA in the culture medium and coating
40
41
42 solution were 7.2 mg/ml and 8.0 mg/ml, respectively, this is much greater than 1.0 mg/ml and
43
44
45 therefore quickly saturates the discs.

46
47
48 The amount of adsorbed BSA on original discs increased with increasing incubation period
49
50
51 and reached similar levels as the BSA-adsorbed discs after 6 h of incubation. This suggests
52
53
54 that amount of protein (mainly BSA) required to saturate the disc was present in the culture
55
56
57 medium and adsorbed onto the original disc after 6 h of incubation. Importantly, a significant

1
2
3
4 difference was observed in the amount of BSA adsorbed in the original disc and BSA-coated
5
6
7 disc after a 3 h incubation period. Therefore, we should pay attention to the initial cell
8
9
10 response between original disc and BSA-adsorbed disc after 3 h in culture.

11 12 13 14 15 **3.3 Adhesion, Spreading, and Proliferation of MC3T3-E1 Cells on Substrates**

16
17
18 Figure 4 shows the number of MC3T3-E1 cells adhered to HA (a) and α -Al₂O₃ discs (b).
19
20
21 After 1 h, the number of cells adhered was approximately 3×10^3 cells/disc on the original
22
23
24 HA disc, this remained constant at later time points. The cell number on BSA-adsorbed HA
25
26
27 discs increased with increasing incubation periods and reached the same as the original HA
28
29
30 disc within 6 h. For the original α -Al₂O₃ discs, few adhered cells were observed after 3 h, and
31
32
33 at 6 h there were approximately 1×10^3 cells/disc. The BSA-adsorbed α -Al₂O₃ discs exhibited
34
35
36 an extremely low number of cells and this did not increased even after 6 h of incubation.
37
38
39 Taken together, these results indicate that BSA adsorption on HA and α -Al₂O₃ inhibits
40
41
42 adhesion of MC3T3-E1 cells [10]. According to Figure 3, saturated adsorption of protein
43
44
45 (mainly BSA) on original HA and α -Al₂O₃ discs takes around 6 h. On the other hand,
46
47
48 MC3T3-E1 cells adhered to original HA within 1 h (see Fig. 4(a)), and they adhered to
49
50
51 original α -Al₂O₃ after more than 6 h (see Fig. 4(b)). This implies that osteoblasts might
52
53
54 adhere to HA before sufficient adsorption of albumin and adhere to α -Al₂O₃ after sufficient
55
56
57 adsorption of albumin.
58
59
60

1
2
3
4 As shown in figure 5, we measured the maximum cell length of MC3T3-E1 cells adhered
5
6
7 to original HA discs and BSA-adsorbed HA discs using fluorescent microscopic images of
8
9
10 MC3T3-E1 cells after treating cells with FDA. The maximum cell length on the original HA
11
12 disc gradually increased with increasing culture periods with a maximum length of ~80 μm
13
14 after 6 h of incubation. In contrast, the maximum length of cells on the BSA-adsorbed HA
15
16 discs was only ~20 μm after 6 h. The number of MC3T3-E1 cells adhered to $\alpha\text{-Al}_2\text{O}_3$ discs
17
18 was extremely low as shown in Fig. 4(b), and therefore, was unable to be statistically
19
20 analyzed.
21
22
23
24
25

26
27 We utilized fluorescent microscopic images of MC3T3-E1 cells on $\alpha\text{-Al}_2\text{O}_3$ discs to
28
29 investigate the morphology of the adhered cells. Figure 6 shows representative fluorescence
30
31 microphotographs of adhered MC3T3-E1 cells on original $\alpha\text{-Al}_2\text{O}_3$ discs (a) and
32
33 BSA-adsorbed $\alpha\text{-Al}_2\text{O}_3$ discs (b). Some cell spreading was observed on the original disc but
34
35 almost only spherical cells were observed on the BSA-adsorbed disc. These results suggest
36
37 that BSA adsorption inhibits the spreading of MC3T3-E1 cells on both HA and $\alpha\text{-Al}_2\text{O}_3$
38
39 coated discs. Therefore, we can speculate that adsorption of albumin might inhibit the
40
41 adhesion and spreading of osteoblast cells, irrespective of the osteoconductivity of materials.
42
43
44
45
46
47
48
49

50 Figure 7 shows the proliferation levels of MC3T3-E1 cells on HA (a) and $\alpha\text{-Al}_2\text{O}_3$ discs (b).
51
52 Both the original HA discs and BSA-adsorbed HA discs exhibited decent cell proliferation
53
54 without any significant difference between the two. Original $\alpha\text{-Al}_2\text{O}_3$ discs and
55
56
57
58
59
60

1
2
3
4 BSA-adsorbed α -Al₂O₃ discs exhibited cell proliferation similar to HA discs over the 7 d
5
6
7 incubation, however, in later incubation periods, the DNA concentration was nearly constant.
8
9
10 This might be because the surface was saturated with adhered cells by 14 d of incubation.
11
12 Notably, no significant difference in the rate of cell proliferation was observed between cells
13
14 on the original α -Al₂O₃ discs or BSA-adsorbed α -Al₂O₃ discs. This suggests that BSA
15
16 adsorption does not affect proliferation of osteoblast cells, irrespective of substrate type.
17
18
19

20
21 Effects of adsorbed BSA on MC3T3-E1 cell response are summarized in left column of
22
23 Table 2. Adsorbed BSA inhibited adhesion and spreading of MC3T3-E1 cells (see Figs. 4 - 6)
24
25 but it hardly affects MC3T3-E1 cell proliferation (see Fig. 7), no matter the substrate type.
26
27 However, for HA, we suggest that the inhibition effect of BSA is decreased because
28
29 MC3T3-E1 cells adhered to HA before sufficient adsorption of BSA. This can be elucidated
30
31 from the results in Fig. 3(a) and 4(a). These data suggest that the quick adherence of
32
33 osteoblast cells might play an important role HA osteoconductivity.
34
35
36
37
38
39
40
41
42
43

44 **3.4 Adhesion, Spreading, and Proliferation of RAW264.7 Cells on Substrates**

45
46
47 Figure 8 shows the number of RAW264.7 cells that were adhered to the HA (a) and
48
49 α -Al₂O₃ discs (b). There was no significant difference in cell number between the original HA
50
51 disc and BSA-adsorbed HA disc. The cell number increased with increasing incubation period
52
53 for original α -Al₂O₃ disc, but reached 1×10^3 cells/disc after 1 h and became almost constant
54
55
56
57
58
59
60

1
2
3
4 after longer incubation periods (up to 6 h) for BSA-adsorbed α -Al₂O₃ discs. This result
5
6 indicates that adsorbed albumin inhibits the adhesion of monocyte-macrophage lineage cells
7
8 on α -Al₂O₃ but not on HA.
9

10
11
12 Figure 9 shows the maximum length of RAW264.7 cells adhered to HA (a) and α -Al₂O₃
13
14 discs (b). All samples revealed a maximum cell length of ~20 μ m, irrespective of incubation
15
16 period. This might be because RAW264.7 cells tended to maintain a spherical shape after
17
18 adherence to substrates. These results suggest that adsorbed albumin hardly affects the
19
20 spreading of monocyte-macrophage lineage cells both on HA and α -Al₂O₃.
21
22
23
24
25
26

27 Figure 10 shows proliferation levels of RAW264.7 cells on HA (a) and α -Al₂O₃ discs (b).
28
29 The amount of proliferation increased with increasing incubation periods (up to 7 d) for both
30
31 original HA discs and BSA-adsorbed HA discs. At 14 d incubation, proliferation levels were
32
33 constant for the original HA disc but decreased for BSA-adsorbed HA disc. Similar results
34
35 were reported in a previous study [16] although the detailed mechanism behind this is unclear.
36
37 There was no statistical difference in proliferation between the original HA disc and
38
39 BSA-adsorbed HA disc at the same incubation period. The proliferation levels increased with
40
41 increasing incubation periods up to 14 days for both the original α -Al₂O₃ discs and
42
43 BSA-adsorbed α -Al₂O₃ discs. Moreover, there was no statistical difference between the
44
45 original α -Al₂O₃ disc and BSA-adsorbed α -Al₂O₃ disc, irrespective of incubation periods.
46
47
48 This suggests that adsorbed albumin hardly affects the proliferation of monocyte-macrophage
49
50
51
52
53
54
55
56
57
58
59
60

1
2
3
4 lineage cells on both HA and α -Al₂O₃ substrates.
5

6
7 The effects of adsorbed BSA on the RAW264.7 cell response are summarized in right
8
9 column of Table 2. Adsorbed BSA inhibits adhesion of RAW264.7 cells on α -Al₂O₃ but not
10
11 on HA (see Fig. 8), whereas it hardly affected the spreading and proliferation of RAW264.7
12
13 cells on both HA and α -Al₂O₃ substrates (see Figs. 9 and 10). These results indicate that the
14
15 initial adhesion of monocyte-macrophage lineage cells is inhibited by BSA adsorbed on
16
17 α -Al₂O₃ but not by BSA adsorbed on HA. While a detail mechanism remains unclear, we
18
19 speculate that the adsorption of BSA on HA plays some role in the cell response [8,17].
20
21
22
23
24
25
26

27 Figure 11 is a schematic describing the relationship of albumin adsorption and adhesion of
28
29 osteoblast cells and monocyte-macrophage lineage cells on HA and α -Al₂O₃ substrates after
30
31 implantation. Immediately after implantation, osteoblast cells, together with
32
33 monocyte-macrophage lineage cells, can adhere to HA prior to excessive albumin adsorption
34
35 (stage 1), monocyte-macrophage lineage cells can further adhere to HA though the
36
37 specifically adsorbed albumin (stages 2 and 3), resulting in osteoconductivity. In contrast, the
38
39 osteoblast cells cannot adhere to α -Al₂O₃ due to the inhibition effect of adsorbed albumin
40
41 immediately after implantation (stage 1). Next, some monocyte-macrophage lineage cells
42
43 adhere to α -Al₂O₃ (stage 2) but osteoblasts cannot further adhere on α -Al₂O₃ (stage 3), this
44
45 results in the non-osteoconductivity. In conclusion, the adsorption behavior of albumin should
46
47 be taken into account when considering the osteoconductivity of artificial materials. We
48
49
50
51
52
53
54
55
56
57
58
59
60

1
2
3 speculate that the specific orientation and arrangement of adsorbed albumin on HA might play
4
5
6 some role in osteoconductivity [8,17] although further investigation relating to the details of
7
8
9 this orientation and arrangement is still required.
10
11
12
13

14 15 **4. Summary** 16

17
18 We investigated effect of adsorbed BSA on responses of osteoblast-like MC3T3-E1 cells
19
20 and RAW264.7 macrophages. The adsorbed BSA inhibited adhesion and spreading of
21
22 MC3T3-E1 cells, but it hardly affected the proliferation of MC3T3-E1 cells on both HA and
23
24 α -Al₂O₃. This suggests that MC3T3-E1 cells quickly adhered to original HA before sufficient
25
26 adsorption of BSA. The adsorbed BSA also inhibits adhesion of RAW264.7 cells on α -Al₂O₃
27
28 but not on HA, whereas it does not affected the spreading and proliferation of RAW264.7
29
30 cells on both HA and α -Al₂O₃ substrates. These results indicate that BSA adsorbed on HA
31
32 induces a different cell response than α -Al₂O₃. Moreover, the quick adherence of osteoblast
33
34 cells and monocyte-macrophage lineage cell likely plays a role in HA osteoconductivity.
35
36
37
38
39
40
41
42
43
44
45
46

47 **References** 48

- 49
50 [1] Jarcho M, Kay JF, Drobeck HP, Doremus RH. Tissue Cellular and Subcellular Events at
51
52 Bone-ceramic Hydroxyapatite Interface. *J. Bioeng.* 1977;2:79-92, 1977.
53
54
55
56 [2] Aoki H, Kato K, Tabata T. Osteocompatibility of apatite ceramics in dog's mandibles.
57
58
59
60

- 1
2
3
4 Rep. Inst. Med. Dent. Eng. Japan 1977;11:33-35.
5
6
7 [3] Hulbert SF. The use of alumina and zirconia in surgical implants, in: L.L. Hench, J.
8
9 Wilson (Eds.), An Introduction to Bioceramics. Singapore: World Scientific; 1993. 25–40
10
11 p.
12
13
14
15 [4] Puleo DA, Nanci A. Understanding and controlling the bone implant interface.
16
17 Biomaterials 1999; 20:2311-2321.
18
19
20
21 [5] Nakamura M, Sekijima Y, Nakamura S, Kobayashi T, Niwa K, Yamashita K., Role of
22
23 blood coagulation components as intermediators of high osteoconductivity of electrically
24
25 polarized hydroxyapatite. J. Biomed. Mater. Res. A 2006;70:627-634, 2006.
26
27
28
29
30 [6] Castner DG, Ratner BD. Biomedical surface science: Foundations to frontiers. Surface
31
32 Science 2002;500:28-60.
33
34
35
36 [7] Tirrell M, Kokkoli E, Biesalski M. The role of surface science in bioengineered materials.
37
38 Surface Science 2002;500: 61-83.
39
40
41
42 [8] Hayashi J, Kawashita M, Miyazaki T, Kamitakahara M, Ioku K, Kanetaka H. Comparison
43
44 of adsorption behavior of bovine serum albumin and osteopontin on hydroxyapatite and
45
46 alumina. Phosphorus Res. Bull 2012;26:23-28.
47
48
49
50 [9] Mavropoulos E, Costa AM, Costa LT, Achete CA, Mello A, Granjeiro AM, Rossi AM.
51
52 Adsorption and bioactivity studies of albumin onto hydroxyapatite surface. Colloids Surf.
53
54 B: Biointerfaces 2011;83: 1-9.
55
56
57
58
59
60

- 1
2
3
4 [10]Bernards MT, Qin C, Ratner BD, Jiang S. Adhesion of MC3T3-E1 cells to bone
5
6 sialoprotein and bone osteopontin specifically bound to collagen I. *J. Biomed. Mater. Res.*
7
8
9
10 A 2008;86:779-787.
11
- 12 [11]Bernards MT, Qin C, Jiang S, MC3T3-E1 cell adhesion to hydroxyapatite with adsorbed
13
14 bone sialoprotein, bone osteopontin, and bovine serum albumin. *Colloids Surf. B:*
15
16
17
18 *Biointerfaces* 2008; 64:236-247.
19
- 20 [12]Ming L, Chen K, Xian CJ. Functions and action mechanisms of flavonoids genistein and
21
22
23
24 icariin in regulating bone remodeling. *J. Cell. Physiol.* 2013;228:513-521.
25
26
- 27 [13]Kajiya M, Giro G, Taubman MA, Han X, Mayer MP, Kawai T. Role of periodontal
28
29
30
31 pathogenic bacteria in RANKL-mediated bone destruction in periodontal disease. *J. Oral*
32
33
34 *Microbiol.* 20120;2:5532-5547.
35
- 36 [14]Aeschlimann D, Evans B. The vital osteoclast: how is it regulated? *Cell Death Differ.*,
37
38
39
40 2004;11:S5-S7.
41
- 42 [15]Bradford MM. A rapid and sensitive method for the quantitation of microgram quantities
43
44
45
46
47 of protein utilizing the principle of protein-dye binding. *Anal. Biochem.* 1976;72:
48
49 248-254.
50
- 51 [16]Xia Z, Grover LM, Huang Y, Adamopoulos IE, Gbureck U, Triffitt JT, Shelton RM,
52
53
54
55
56 Barralet JE. In vitro biodegradation of three brushite calcium phosphate cements by a
57
58
59
60 macrophage cell-line. *Biomaterials* 2006;27:4557-4565.

1
2
3
4 [17]M. Kawashita M, Hayashi J, Li Z, Miyazaki T, Hashimoto H, Hihara H, Kanetaka H,
5
6
7 Adsorption characteristics of bovine serum albumin onto alumina with a specific
8
9
10 crystalline structure. J. Mater. Sci.: Mater. Med. submitted.
11
12
13
14
15
16
17
18
19
20
21
22
23
24
25
26
27
28
29
30
31
32
33
34
35
36
37
38
39
40
41
42
43
44
45
46
47
48
49
50
51
52
53
54
55
56
57
58
59
60

Figure captions

- 1
2
3
4
5
6
7
8
9
10
11
12
13
14
15
16
17
18
19
20
21
22
23
24
25
26
27
28
29
30
31
32
33
34
35
36
37
38
39
40
41
42
43
44
45
46
47
48
49
50
51
52
53
54
55
56
57
58
59
60
- Figure 1 TF-XRD patterns of (a) HA disc and (b) α -Al₂O₃ disc.
- Figure 2 SEM photographs of (a) HA disc and (b) α -Al₂O₃ disc.
- Figure 3 Time-dependent adsorption of protein on (a) HA discs and (b) α -Al₂O₃ discs. Five samples for each experiment were analyzed for the acquired data (mean \pm SE, Student's t-test, * $P < 0.05$, ** $P < 0.01$, n. s.: not significant).
- Figure 4 Number of MC3T3-E1 cells adhered on HA discs (a) and α -Al₂O₃ discs (b) (mean \pm SE, Holm's test, * $P < 0.05$, n. s.: not significant).
- Figure 5 Maximum length of MC3T3-E1 cells adhered on original HA disc and BSA-adsorbed HA discs (mean \pm SE, Holm's test, ** $P < 0.01$).
- Figure 6 Representative fluorescent microscopic images of MC3T3-E1 cells adhered to original α -Al₂O₃ discs (a) and BSA-coated α -Al₂O₃ discs (b).
- Figure 7 Proliferation of MC3T3-E1 cells on HA discs (a) and α -Al₂O₃ discs (b) (mean \pm SE, Holm's test, n.s.: not significant).
- Figure 8 Number of RAW264.7 cells adhered to HA discs (a) and α -Al₂O₃ discs (b) (mean \pm SE, Holm's test, * $P < 0.05$, n. s.: not significant).
- Figure 9 Maximum length of RAW264.7 cells adhered to HA discs (a) and α -Al₂O₃ discs

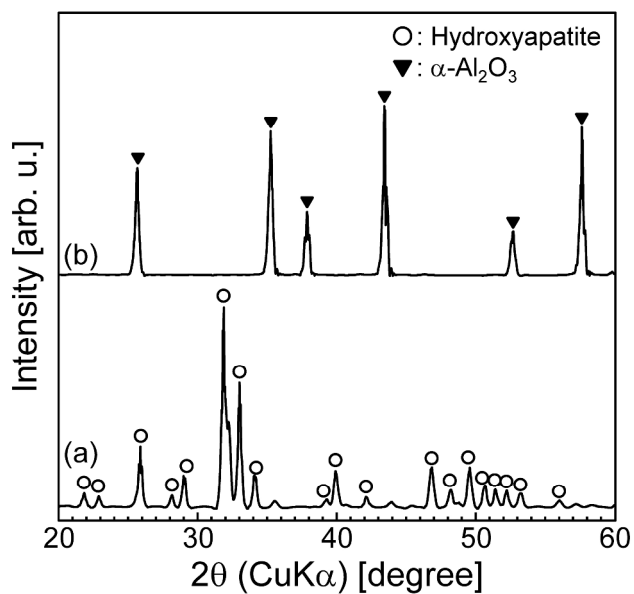
1
2
3
4 (b) (mean \pm SE, Holm's test, n. s.: not significant).
5

6
7 Figure 10 Proliferation of RAW264.7 cells on HA discs (a) and α -Al₂O₃ discs (b) (mean \pm
8
9 SE, Holm's test, **P* < 0.05, n. s.: not significant).
10

11
12 Figure 11 Schematic of potential mechanism behind albumin adsorption and adhesion of
13
14 osteoblast cells and monocyte-macrophage lineage cells to HA and α -Al₂O₃ after
15
16 implantation.
17
18
19

20
21
22
23
24 Table 1 Quantitative results of roughness measurements. Five points on the disc for each
25
26 experiment were analyzed for the acquired data.
27
28

29
30 Table 2 Effects of BSA adsorption on MC3T3-E1 and RAW264.7 cells response to HA or
31
32 α -Al₂O₃ substrates.
33
34
35
36
37
38
39
40
41
42
43
44
45
46
47
48
49
50
51
52
53
54
55
56
57
58
59
60

Figure 1 M. Kawashita *et al.*

TF-XRD patterns of (a) HA disc and (b) α -Al $_2$ O $_3$ disc.
297x420mm (300 x 300 DPI)

1
2
3
4
5
6
7
8
9
10
11
12
13
14
15
16
17
18
19
20
21
22
23
24
25
26
27
28
29
30
31
32
33
34
35
36
37
38
39
40
41
42
43
44
45
46
47
48
49
50
51
52
53
54
55
56
57
58
59
60

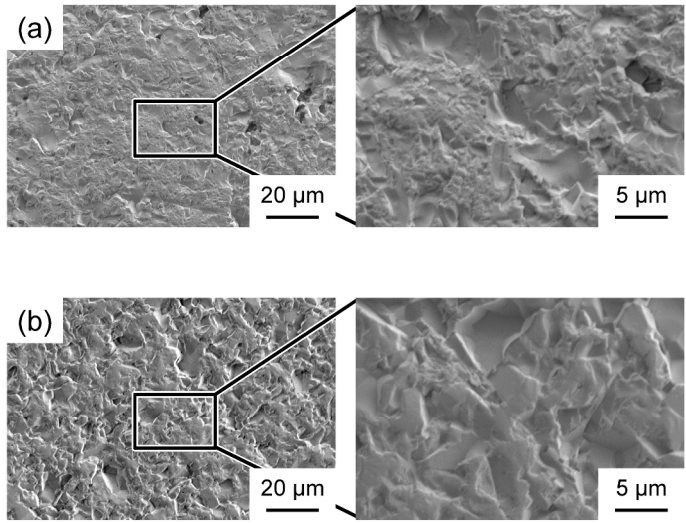
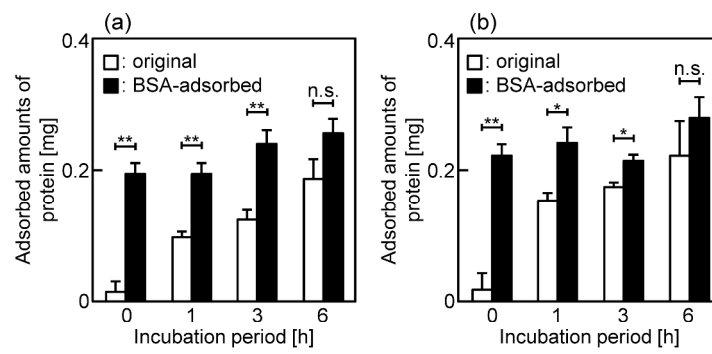


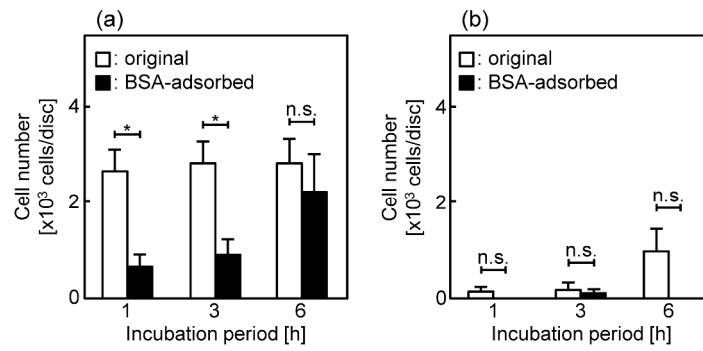
Figure 2 M. Kawashita *et al.*

SEM photographs of (a) HA disc and (b) α -Al₂O₃ disc.
297x420mm (300 x 300 DPI)

Figure 3 M. Kawashita *et al.*

Time-dependent adsorption of protein on (a) HA discs and (b) α -Al₂O₃ discs. Five samples for each experiment were analyzed for the acquired data (mean \pm SE, Student's t-test, * P < 0.05, ** P < 0.01, n. s.: not significant).

297x420mm (300 x 300 DPI)

Figure 4 M. Kawashita *et al.*

Number of MC3T3-E1 cells adhered on HA discs (a) and α -Al₂O₃ discs (b) (mean \pm SE, Holm's test, *P < 0.05, n. s.: not significant).

297x420mm (300 x 300 DPI)

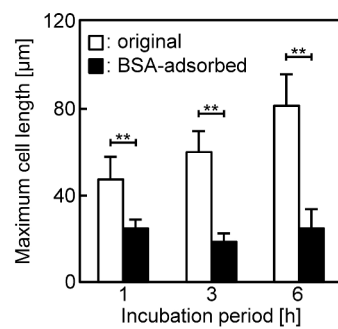


Figure 5 M. Kawashita *et al.*

Maximum length of MC3T3-E1 cells adhered on original HA disc and BSA-adsorbed HA discs (mean \pm SE, Holm's test, **P < 0.01).
297x420mm (300 x 300 DPI)

1
2
3
4
5
6
7
8
9
10
11
12
13
14
15
16
17
18
19
20
21
22
23
24
25
26
27
28
29
30
31
32
33
34
35
36
37
38
39
40
41
42
43
44
45
46
47
48
49
50
51
52
53
54
55
56
57
58
59
60

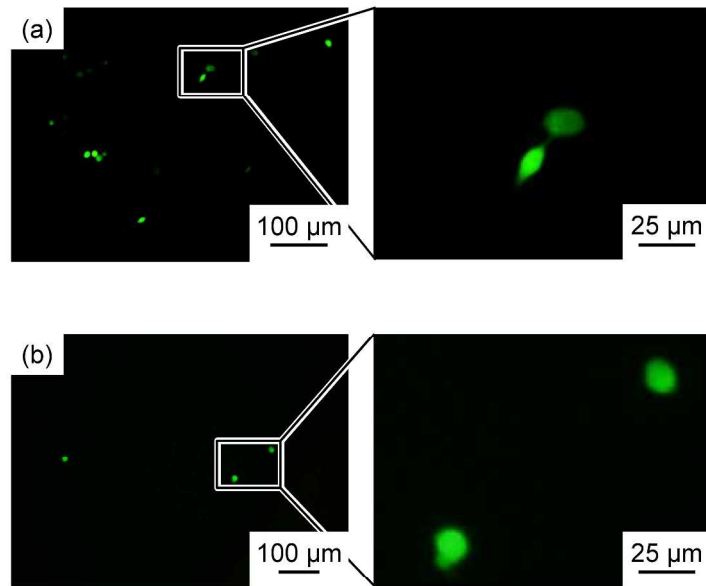


Figure 6 M. Kawashita *et al.*

Representative fluorescent microscopic images of MC3T3-E1 cells adhered to original α -Al₂O₃ discs (a) and BSA-coated α -Al₂O₃ discs (b).
297x420mm (300 x 300 DPI)

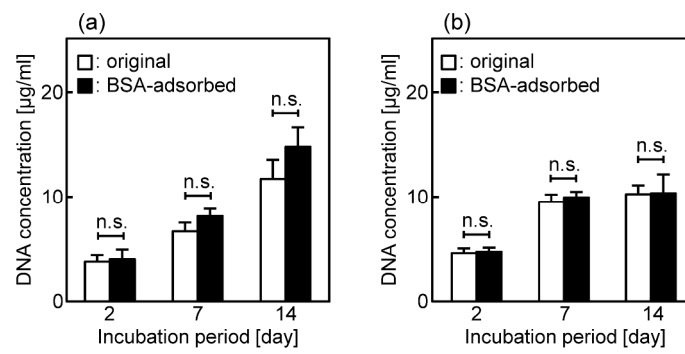
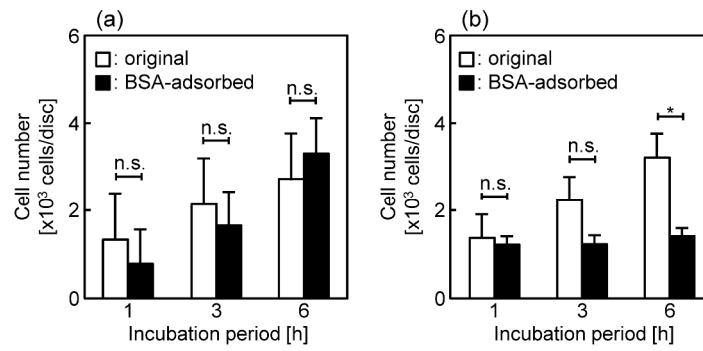


Figure 7 M. Kawashita *et al.*

Proliferation of MC3T3-E1 cells on HA discs (a) and α-Al₂O₃ discs (b) (mean ± SE, Holm's test, n.s.: not significant).

297x420mm (300 x 300 DPI)

Figure 8 M. Kawashita *et al.*

Number of RAW264.7 cells adhered to HA discs (a) and α -Al₂O₃ discs (b) (mean \pm SE, Holm's test, *P < 0.05, n. s.: not significant).
297x420mm (300 x 300 DPI)

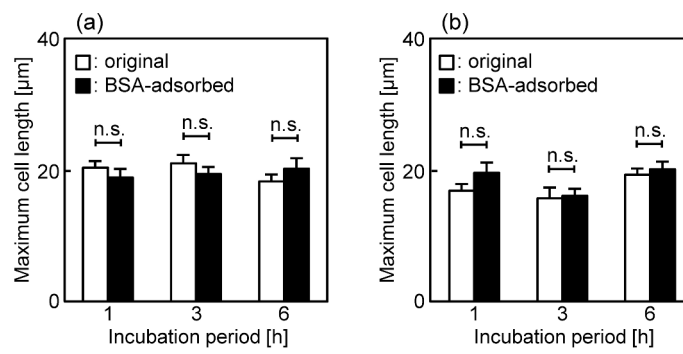
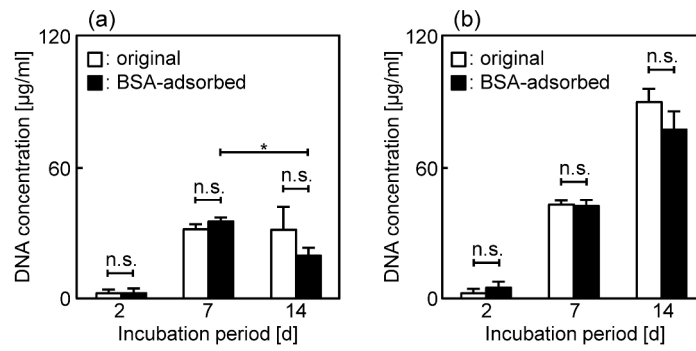


Figure 9 M. Kawashita *et al.*

Maximum length of RAW264.7 cells adhered to HA discs (a) and α-Al₂O₃ discs (b) (mean ± SE, Holm's test, n. s.: not significant).
297x420mm (300 x 300 DPI)

Figure 10 M. Kawashita *et al.*

Proliferation of RAW264.7 cells on HA discs (a) and α -Al₂O₃ discs (b) (mean \pm SE, Holm's test, *P < 0.05, n. s.: not significant).

297x420mm (300 x 300 DPI)

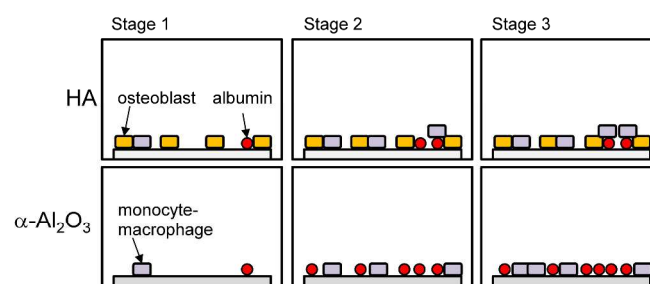


Figure 11 M. Kawashita *et al.*

Schematic of potential mechanism behind albumin adsorption and adhesion of osteoblast cells and monocyte-macrophage lineage cells to HA and α -Al₂O₃ after implantation.
297x420mm (300 x 300 DPI)

Figure 1 Quantitative results of roughness measurements. Five points on the disc for each experiment were analyzed for the acquired data.

disc	Ra [mm]	Ry [mm]	Rz [mm]
HA	2.35 ± 0.14	14.71 ± 1.69	6.61 ± 0.83
$\alpha\text{-Al}_2\text{O}_3$	2.35 ± 0.29	16.93 ± 3.12	7.54 ± 1.58

Table 2 Effects of BSA adsorption on MC3T3-E1 and RAW264.7 cells response to HA or α -Al₂O₃ substrates.

	MC3T3-E1 cell			RAW264.7 cell		
	Adhesion	Spreading	Proliferation	Adhesion	Spreading	Proliferation
HA	Inhibited	Inhibited	Not affected	Not affected	Not affected	Not affected
α -Al ₂ O ₃	Inhibited	Inhibited	Not affected	Inhibited	Not affected	Not affected